



Shahrood University of
Technology



Iranian Society of
Mining Engineering
(IRSM)

Optimizing Hybrid Photocatalytic-ozonation for Offshore Produced Water Treatment

Masoud Rabeian and Farhad Qaderi*

Faculty of Civil Engineering, Babol Noshirvani University of Technology, Babol, Iran

Article Info

Received 5 May 2023

Received in Revised form 11
November 2023

Accepted 21 November 2023

Published online 21 November
2023

DOI: [10.22044/jme.2023.13081.2376](https://doi.org/10.22044/jme.2023.13081.2376)

Keywords

Photocatalytic ozonation

Polycyclic aromatic
hydrocarbons

Offshore produced water

Response surface methodology

Environmental sustainability

Abstract

Offshore produced water (OPW), a type of wastewater rich in hazardous compounds such as polycyclic aromatic hydrocarbons (PAHs), requires effective treatment. This study presents a novel methodology utilizing TiO₂ nanoparticles, ultraviolet (UV) lamps, and ozonation for the degradation of phenanthrene (PHE) from OPW. Various factors including UV lamp power (10W-50W), ozone dose (0.1 mg/L-0.5 mg/L), TiO₂ concentration (0.5 g/m²-2.1 g/m²), ethanol fraction (25%-85%), pH (4.5-10.5), PHE initial concentration (5 mg/L-25 mg/L), and treatment time (15 min-45 min) were systematically investigated to understand their impact on PAH degradation in the OPW. The study employs Response Surface Methodology (RSM) for modeling and optimizing PHE removal efficiency. The results contribute to the development of a mathematical model, and through optimization, optimal conditions are proposed to maximize PHE removal efficiency. Experimental implementation of the optimized conditions in a physical model resulted in an impressive 98% PHE removal efficiency. The identified optimal conditions include UV lamp power of 40 W, ozone dose of 0.5 mg/L, TiO₂ concentration of 2 g/m², ethanol fraction of 25%, pH of 5.2, initial PHE concentration of 15 mg/L, and a treatment time of 40 min. This optimized approach provides valuable insights for efficient and environmentally friendly treatment of PAHs in OPW, emphasizing on the potential for practical application in soil washing effluent treatment.

1. Introduction

Persistent organic chemicals, recognized as pervasive pollutants in the majority of ecosystems [1], pose significant environmental concerns. Polycyclic aromatic hydrocarbons (PAHs), a subgroup of persistent organic pollutants, are particularly noteworthy due to their classification as hazardous substances. These compounds have been globally identified in various environmental compartments such as soil, sludge, and water, stemming from diverse sources including industrial and municipal activities, as well as natural processes. The mutagenic and carcinogenic effects of PAHs contribute to their designation as hazardous pollutants [2].

The sources of PAH pollution in surface waters encompass a range of activities including fossil fuel combustion, coke ovens, metal processing facilities, and hydrocarbon production.

Phenanthrene, a representative PAH compound and a priority pollutant according to the United States Environmental Protection Agency, poses a significant challenge as one of the most widely detected PAHs in contaminated sites [3, 4].

Recent research highlights advanced oxidation processes (AOPs) as effective methods for degrading aromatic compounds like PAHs [5]. The use of the highly reactive hydroxyl radical ($\bullet\text{OH}$) in AOP processes facilitates the oxidation of PAHs into less toxic byproducts, ultimately leading to the formation of H₂O and CO₂ [6].

Ozone, with its high oxidant capacity and disinfection potential, emerges as a viable option for removing compounds like phenanthrene. Ozone treatment can proceed through direct molecular reactions and/or an indirect pathway involving ozone decomposition and the generation of

✉ Corresponding author: F.Qaderi@nit.ac.ir (F. Qaderi)

hydroxyl radicals ($\bullet\text{OH}$). Laboratory experiments such as those conducted by Do-Yun *et al.* on remediation of contaminated soil by ozone, demonstrate its effectiveness in achieving substantial pollutant removal. Factors such as soil pH and moisture content impact the efficiency of PAH oxidation in unsaturated soil during in-situ ozonation, highlighting the need for effective *in situ* treatment technologies employing ozone [7].

For high molecular weight or complex structure PAHs, photocatalytic degradation (photodegradation) emerges as a highly effective technique, aligning with the criteria of being economical, efficient, and environmentally friendly. Recent studies emphasize the applicability of photocatalysis using TiO_2 semiconductor photocatalysts for achieving complete mineralization of organic substrates. TiO_2 , widely employed as a photocatalyst, has demonstrated efficient degradation of various PAHs [8, 9]. However, challenges such as the need for solid-liquid separation post-treatment and susceptibility of suspended catalysts to water matrices have prompted research into immobilization techniques [9].

Co-solvents, particularly alcohols, are frequently used to enhance the desorption of hydrophobic organic compounds including PAHs from soil particles during soil washing. The advantages of using co-solvents include increased pollutant solubility in water, environmental friendliness, simplicity of application, and the ability to be conducted at ambient temperature [1, 6].

In conventional AOP methods, variations in parameters are often tested individually, leading to an increase in the number of experiments. To address this, experimental design methodologies such as Response Surface Methodology (RSM) are employed to optimize effective parameters with a minimal number of experiments. RSM facilitates the quantification of relationships between independent and dependent variables, allowing for the evaluation of variable effects, interactions, and simultaneous impacts. Two primary experimental design methods, Box-Behnken design and central composite design (CCD), are commonly utilized. CCD, with experiments designed at 5 levels, provides more comprehensive information than Box-Behnken design. This study employs the CCD method to optimize the factors influencing the photocatalytic ozonation degradation behavior of phenanthrene in co-solvent, providing a robust approach to the design and formulation of new processes [9].

As a consequence of these considerations, phenanthrene has been selected as a model compound for the investigation of its advanced oxidation through the synergistic combination of ozone and ultraviolet (C type) radiation, along with a semi-conductor TiO_2 , in a process termed photocatalytic ozonation ($\text{TiO}_2/\text{UVC}/\text{O}_3$), in the presence of co-solvent ethanol. This study seeks to elucidate the factors influencing the photocatalytic ozonation degradation of phenanthrene in co-solvent, employing the CCD method for modeling and optimization within the framework of Response Surface Methodology (RSM).

2. Materials and methods

2.1. Chemicals

All chemical used in the experiments were analytic grade reagents. Phenanthrene (PHE) was selected as a representative PAH due to its low volatilization, and it was purchased from Aldrich (WI, USA) with purity greater than 99%. A commercial TiO_2 Degussa P25 (70% anatase and 30% rutile) was used as the catalyst with an average particle size of 30 nm and BET surface area of $50 \text{ m}^2\text{g}^{-1}$, according to the manufacturer. Absolute ethyl alcohol (Sigma-Aldrich, 99.5%) was used as co-solvent. Dichloromethane (supplied by Sigma-Aldrich, USA) was used for aqueous sample extraction. Furthermore 0.5M H_2SO_4 and 1M NaOH (Merck) were used to adjust the initial solution pH.

2.2. Preparation of samples

The model solutions were prepared in different PHE initial concentration and with different ethanol fraction, according to designed experiments by the Design Expert software (version 10.0.7). Different PHE concentrations were prepared in mixture of distillate ethanol/water (in different ratio). The solution completely stirred at a dark cage for 24 h and room temperature. The initial pH was adjusted by 0.5 M H_2SO_4 or 1M NaOH, and it was uncontrolled during the process.

2.3. Photocatalytic ozonation of phenanthrene

Figure 1 shows the experimental setup of photocatalytic ozonation reactor. Five coated plates with TiO_2 nanoparticles were placed at bottom and four sides of reactor. Five 10 W UV lamp (253.7 nm, light intensity about $6 \times 10^{-7} \text{ L}^{-1}\text{s}^{-1}$) were used for photocatalytic process, and at the bottom of reactor, there was a porous for ozone injection. Amount of nanoparticles, time of photocatalytic ozonation process, power of lamps, ozonation

dose, and PHE initial concentration were set due to designed experiments, as independent variables. A water bath was used to keep the system at ambient temperature to prevent thermal catalytic effect.

2.4. Immobilization of catalysts

The immobilization of catalysts on glass slides was conducted using a heat-attached method. Due to designed experiments, an amount of TiO_2 was dispersed into ethanol. The glass plate was pre-treated with dilute hydrofluoric acid (0.1 mol. L^{-1}) and 0.01 mol. L^{-1} sodium hydroxide solution. After these processes, the number of OH group increased and the TiO_2 immobilization efficiency enhanced. The solution of TiO_2 was sonicated (by vCLEAN1 – L2 Ultrasonic Cleaner) with 100% amplitude for 30 min and at a frequency of 30 kHz. After washing glass with distilled water, both sides of the glass were dipped into TiO_2 solution, and then dried at 30°C . After drying, the glass plate was fired at 450°C . After 60 min, plates were washed with distilled

water for removal of weakly attached TiO_2 P-25 nanoparticles.

2.5. PAHs extraction processes

Phenanthrene in solution was extracted using hexane with a liquid-liquid extraction method, concentrated with a rotary evaporator, and cleaned up with a silica solid phase extraction column. All samples were quantified by a GC-FID system [6].

2.6. GC analysis of PAHs

The concentration of PHE was carried out using TG 2552 GC system, equipped with a flame ionization detector (FID) was operated in splitless mode and manual injection. The injection volume was $1 \mu\text{L}$, and the detector temperature was 300°C . The injector temperature was set at 290°C . The oven temperature was set initially at 50°C (held for 1 min), increased to 205°C at $10^\circ\text{C}/\text{min}$, finally at $25^\circ\text{C}/\text{min}$ increased to 300°C , and held for 5 min at this temperature [6].

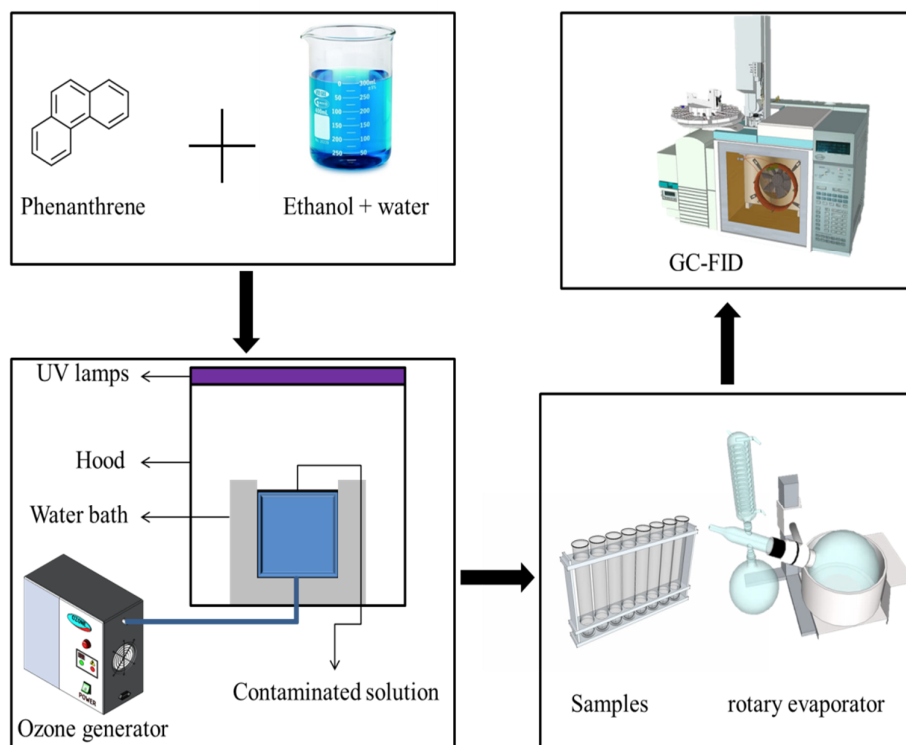


Figure 1. Schematic representation of the photocatalytic ozonation process setup.

2.7. Experimental design

For designing experiments and statistical analyzing of results, the Design Expert software

(version 10.0.7) has been used. RSM¹ was performed using the CCD² method to investigate the effects of seven independent variables on dependent variable. Finally, it has been achieved a

¹ Response Surface Methodology

² Central Composite Design

mathematical model for PHE removal efficiency, for optimization of independent variables in order to achieve maximum removal of phenanthrene. Among the linear, quadratic, and special models, a quadratic model has been considered for results of this study.

The independent variables of this study were PHE initial concentration, solution pH, ethanol fraction, UV power, ozone dose, TiO₂ concentration, and treatment time, and the dependent variable was phenanthrene removal efficiency. The design conditions are presented in Table 1.

Table 1. Independent variables and their levels for central composite design.

Design points	Unit	Level 1 (min)	Level 2	Level 3 (mid)	Level 4	Level 5 (max)
Ethanol ratio	%	10	25	55	85	100
initial concentration	mg/l	0	5	15	25	30
pH		3	4.5	7.5	10.5	12
UV power	W	0	10	30	50	60
O ₃ dosage	mg/L	0	0.1	0.3	0.5	0.6
TiO ₂ concentration	g/m ²	0.1	0.5	1.3	2.1	2.5
Treatment time	min	0	15	45	75	90

Table 2. CCD for the study of seven experimental variables and results.

Run	UV	O ₃	TiO ₂	t	pH	EW	C	RE	Run	UV	O ₃	TiO ₂	t	pH	EW	C	RE
1	10	0.5	2.1	75	10.5	25	15.65	82.85	53	50	0.5	2.1	15	4.5	25	15.65	80.12
2	10	0.5	0.5	75	10.5	25	0.85	45.97	54	30	0.3	0.1	45	7.5	55	13.94	61.3
3	50	0.1	0.5	75	4.5	25	0.85	45.65	55	10	0.5	0.5	15	4.5	25	15.65	57.45
4	50	0.1	0.5	75	10.5	85	24.64	41.39	56	30	0.3	2.5	45	7.5	55	13.94	78.48
5	50	0.1	2.1	15	10.5	85	2.25	27.17	57	10	0.1	2.1	15	10.5	85	2.25	13.13
6	10	0.1	0.5	15	10.5	25	0.85	9.23	58	50	0.1	2.1	15	4.5	85	2.25	30.7
7	50	0.1	2.1	75	4.5	25	15.65	76.14	59	10	0.1	0.5	75	10.5	25	15.65	40.73
8	50	0.5	2.1	75	10.5	85	24.64	73.35	60	10	0.5	0.5	15	10.5	25	0.85	34.55
9	50	0.1	2.1	15	10.5	25	0.85	47.09	61	50	0.1	0.5	75	10.5	25	0.85	38.23
10	30	0.3	1.3	90	7.5	55	13.94	60.42	62	30	0.3	1.3	45	7.5	55	13.94	61.22
11	50	0.1	2.1	15	10.5	25	15.65	63.95	63	30	0.3	1.3	45	7.5	10	8.55	59.64
12	10	0.1	0.5	75	10.5	85	2.25	22.36	64	10	0.1	0.5	75	4.5	25	0.85	27.21
13	10	0.1	0.5	75	10.5	25	0.85	18.51	65	50	0.5	0.5	15	4.5	85	24.64	50.47
14	10	0.5	0.5	75	4.5	85	24.64	58.47	66	50	0.1	0.5	15	4.5	85	24.64	36.53
15	50	0.1	2.1	75	4.5	85	24.64	52.49	67	10	0.1	2.1	75	10.5	25	15.65	51.81
16	50	0.5	2.1	15	10.5	25	15.65	95.84	68	50	0.5	0.5	15	10.5	85	2.25	43.84
17	10	0.5	2.1	75	10.5	85	2.25	46.02	69	10	0.5	0.5	75	10.5	85	2.25	40.76
18	50	0.1	0.5	15	10.5	25	15.65	43.39	70	50	0.5	0.5	15	4.5	25	15.65	77.05
19	10	0.1	2.1	75	4.5	85	24.64	47.81	71	10	0.1	0.5	75	4.5	85	2.25	30.81
20	30	0.3	1.3	45	7.5	55	13.94	58.95	72	10	0.5	0.5	15	4.5	25	0.85	41.32
21	50	0.5	0.5	75	10.5	85	2.25	57.8	73	50	0.1	2.1	75	10.5	85	2.25	36.42
22	10	0.5	2.1	75	4.5	25	15.65	83.03	74	50	0.5	0.5	75	4.5	85	24.64	64.87
23	30	0.6	1.3	45	7.5	55	13.94	79.9	75	30	0.3	1.3	45	7.5	55	13.94	55.64
24	10	0.5	0.5	15	4.5	85	24.64	45.35	76	10	0.1	0.5	75	4.5	25	15.65	49.59
25	50	0.5	0.5	15	10.5	25	15.65	71.41	77	50	0.5	0.5	75	4.5	25	0.85	79.74
26	10	0.1	2.1	15	10.5	25	0.85	21.74	78	10	0.5	2.1	15	4.5	85	24.64	51.23
27	10	0.5	0.5	75	10.5	85	24.64	51.76	79	50	0.1	2.1	75	10.5	85	24.64	48.77
28	10	0.1	2.1	15	4.5	85	24.64	39.41	80	10	0.5	2.1	75	10.5	85	24.64	58.76
29	50	0.1	2.1	15	10.5	85	24.64	39.04	81	10	0.1	2.1	75	4.5	25	0.85	33.46
30	50	0.1	0.5	75	10.5	25	15.65	54.27	82	50	0.1	2.1	75	4.5	85	2.25	39.9
31	10	0.1	2.1	75	10.5	25	0.85	28.44	83	10	0.5	2.1	15	10.5	85	24.64	48.17
32	30	0.3	1.3	45	3	55	13.94	58.66	84	50	0.1	2.1	15	4.5	85	24.64	42.81
33	10	0.5	0.5	75	4.5	25	0.85	52.68	85	50	0.1	0.5	75	4.5	25	15.65	61.84
34	10	0.5	0.5	75	4.5	85	2.25	47.22	86	50	0.1	0.5	75	4.5	85	24.64	48.79
35	50	0.1	0.5	15	10.5	25	0.85	27.67	87	50	0.5	2.1	75	10.5	25	0.85	93.24
36	50	0.1	0.5	15	10.5	85	2.25	18.94	88	10	0.5	0.5	15	4.5	85	2.25	34.59
37	10	0.1	2.1	15	4.5	85	2.25	17.94	89	10	0.1	2.1	75	4.5	85	2.25	25.86
38	50	0.1	2.1	75	4.5	25	0.85	58.8	90	10	0.5	2.1	15	4.5	25	0.85	56.65
39	50	0.5	2.1	15	4.5	25	0.85	89.34	91	50	0.1	0.5	15	4.5	85	2.25	26.16

Table 2. Continued.

Run	UV	O ₃	TiO ₂	t	pH	EW	C	RE	Run	UV	O ₃	TiO ₂	t	pH	EW	C	RE
40	10	0.1	2.1	75	4.5	25	15.65	56.98	92	50	0.5	0.5	75	4.5	25	15.65	90.01
41	10	0.1	0.5	75	10.5	85	24.64	42.33	93	50	0.1	0.5	75	4.5	85	2.25	37.94
42	10	0.1	0.5	15	4.5	25	15.65	40.04	94	30	0.3	1.3	45	7.5	55	13.94	59.23
43	10	0.5	2.1	15	4.5	25	15.65	73.93	95	10	0.5	0.5	15	10.5	25	15.65	50.53
44	30	0.3	1.3	45	12	55	13.94	50.78	96	10	0.5	2.1	75	10.5	25	0.85	62.41
45	50	0.5	0.5	15	4.5	85	2.25	49.07	97	10	0.5	2.1	15	10.5	85	2.25	35.91
46	50	0.1	2.1	15	4.5	25	0.85	50.87	98	10	0.1	0.5	15	10.5	85	2.25	11.8
47	30	0.3	1.3	0	7.5	55	13.94	44.56	99	30	0	1.3	45	7.5	55	13.94	44.68
48	50	0.1	0.5	75	10.5	85	2.25	30.77	100	0	0.3	1.3	45	7.5	55	13.94	51.36
49	10	0.1	2.1	15	4.5	25	0.85	26.81	101	10	0.1	0.5	15	4.5	85	24.64	40.03
50	10	0.1	0.5	15	10.5	25	15.65	31.13	102	10	0.5	2.1	75	4.5	85	24.64	61.77
51	30	0.3	1.3	45	7.5	100	15.33	42.4	103	50	0.5	0.5	75	10.5	25	0.85	74.32
52	60	0.3	1.3	45	7.5	55	13.94	74.42	104	30	0.3	1.3	45	7.5	55	13.94	60.14
105	10	0.1	2.1	75	10.5	85	24.64	42.81	129	10	0.5	0.5	75	4.5	25	15.65	69.13
106	50	0.1	2.1	75	10.5	25	0.85	55.07	130	50	0.5	2.1	75	10.5	85	2.25	69.97
107	10	0.1	0.5	15	4.5	85	2.25	20.31	131	50	0.1	2.1	15	4.5	25	15.65	67.89
108	30	0.3	1.3	45	7.5	55	25.82	53.92	132	10	0.5	2.1	15	10.5	25	0.85	53.58
109	50	0.5	0.5	15	10.5	25	0.85	61.62	133	50	0.5	2.1	75	4.5	85	2.25	71.45
110	10	0.5	0.5	15	10.5	85	24.64	38.6	134	10	0.1	0.5	15	4.5	25	0.85	17.98
111	50	0.1	2.1	75	10.5	25	15.65	72.25	135	50	0.5	2.1	75	4.5	85	24.64	75.08
112	50	0.5	2.1	75	4.5	25	0.85	90.74	136	30	0.3	1.3	45	7.5	55	0.17	40.45
113	50	0.1	0.5	15	10.5	85	24.64	29.07	137	10	0.5	2.1	75	4.5	25	0.85	65.43
114	50	0.5	2.1	15	10.5	85	24.64	61.48	138	30	0.3	1.3	45	7.5	55	13.94	58.36
115	50	0.5	2.1	75	10.5	25	15.65	97.55	139	10	0.1	2.1	15	10.5	85	24.64	34.36
116	10	0.5	2.1	15	4.5	85	2.25	38.73	140	30	0.3	1.3	45	7.5	55	13.94	57.69
117	50	0.1	0.5	15	4.5	25	15.65	51.02	141	10	0.5	0.5	75	10.5	25	15.65	62.26
118	50	0.1	0.5	15	4.5	25	0.85	35.14	142	50	0.5	0.5	75	10.5	25	15.65	84.42
119	50	0.5	0.5	15	10.5	85	24.64	45.01	143	50	0.5	2.1	15	4.5	85	2.25	60.12
120	10	0.1	0.5	15	10.5	85	24.64	31.29	144	50	0.5	2.1	15	10.5	25	0.85	87.55
121	10	0.5	0.5	15	10.5	85	2.25	28.07	145	30	0.3	1.3	45	7.5	55	13.94	59.83
122	50	0.5	2.1	15	4.5	85	24.64	63.26	146	30	0.3	1.3	45	7.5	55	13.94	61.48
123	10	0.5	2.1	15	10.5	25	0.85	53.58	147	50	0.5	2.1	75	4.5	25	15.65	100
124	50	0.5	0.5	15	4.5	25	0.85	67.1	148	30	0.3	1.3	45	7.5	55	13.94	56.99
125	50	0.5	2.1	15	10.5	85	2.25	58.58	149	10	0.1	0.5	75	4.5	85	24.64	51.02
126	10	0.1	2.1	75	10.5	85	2.25	21.1	150	50	0.5	0.5	75	4.5	85	2.25	62.98
127	10	0.1	2.1	15	4.5	25	15.65	50.01	151	10	0.5	2.1	75	4.5	85	2.25	48.79
128	10	0.1	2.1	15	10.5	25	15.65	44.79	152	50	0.5	0.5	75	10.5	85	24.64	59.45

3. Result and Discussion

PHE removal efficiency from solution was considered as the dependent variable. In this study, response surface methodology was employed for association modeling between dependent and independent variables. Thus, statistical analysis of RSM and mathematical model, and also the distinctive effect of each variable on the dependent variable; interaction between the independent

Table 1 the p-value of the model is less than 0.0001. If the p-value of the model is less than 0.05, it means that the model terms are significant, otherwise; if the p-value of the model is greater than 0.1, this indicates the terms that are not significant. Thus the model that was developed in this study is significant [10, 11]. The quality of the developed model can be expressed by the correlation coefficient, which was represented by the R² value. This parameter indicates data variation that is accounted by the model [4, 12].

variable and simultaneous effect of them have been represented, respectively.

3.1. Statistical analysis of RSM

The analysis of variance table (ANOVA) evaluated the RSM model at 95% confidence level (p-value < 0.05). ANOVA results have been shown in Table 5; according to the

The R² value of this study was 99.05%, which means 99.05% of data variations of PHE removal efficiency are explained by the independent variable of the model; in other words, only 0.95% of variations are not explained by this developed model. The adjusted R² modified the R² value by taking into account the number of insignificant terms that are added to the model, and the predicted R² will decrease when there are too many insignificant terms in the model. The difference between adjusted and predicted R² should not be

greater than 0.2, according to a rule of thumb [9, 13].

Table 1. ANOVA results for response surface quadratic model.

Source	Sum of squares	Mean square	F- value	p-value	
Model	5.39	0.20	477.71	< 0.0001	Significant
A- UV	0.53	0.53	1269.44	< 0.0001	
B-Ozone dose	1.34	1.34	3213.50	< 0.0001	
C- TiO ₂	0.36	0.36	852.84	< 0.0001	
D- Time	0.36	0.36	854.37	< 0.0001	
E- pH	0.078	0.078	187.76	< 0.0001	
F- ETW	0.50	0.50	1201.83	< 0.0001	
G- C	0.054	0.054	130.16	< 0.0001	
AB	0.036	0.036	87.00	< 0.0001	
AC	0.020	0.020	48.24	< 0.0001	
AE	2.843E-003	2.843E-003	6.81	0.0102	
AF	0.055	0.055	131.58	< 0.0001	
AG	0.061	0.061	145.33	< 0.0001	
BC	0.018	0.018	43.29	< 0.0001	
BD	2.798E-003	2.798E-003	6.70	0.0108	
BE	5.927E-003	5.927E-003	14.19	0.0003	
BF	0.032	0.032	75.53	< 0.0001	
BG	0.056	0.056	133.46	< 0.0001	
CD	6.458E-003	6.458E-003	15.46	0.0001	
CE	0.016	0.016	37.43	< 0.0001	
CF	0.067	0.067	159.81	< 0.0001	
A ²	2.595E-003	2.595E-003	6.21	0.0140	
B ²	1.747E-003	1.747E-003	4.18	0.0430	
C ²	0.025	0.025	59.56	< 0.0001	
D ²	0.012	0.012	27.77	< 0.0001	
E ²	5.429E-003	5.429E-003	13.00	0.0005	
F ²	0.011	0.011	25.38	< 0.0001	
G ²	0.10	0.10	248.62	< 0.0001	
Residual	0.052	4.177E-004			
Lack of fit	0.049	4.275E-004	1.40	0.2909	Not significant
Pure Error	3.056E-003	3.056E-004			

The adjusted R^2 and the predicted R^2 are 98.84% and 98.62%, respectively, in this study. As shown, adjusted R^2 is close to predicted R^2 , which shows a high significance of the model [5]. Moreover, the adequate precision indicates the signal to noise ratio. A ratio greater than 4 is generally desirable [10, 14, 15]. In this study, ratio of 109.212 indicates an adequate signal. Thus, this model can be used to navigate the design space. The evaluated model adequacy is an important part of data analysis procedure, as it will give poor or misleading result if it is an inadequate fit. The residual model was examined by the approximating model [16].

The other criteria for model validation is lack of fit. The lack of fit F-test describes the deviation of actual points from the fitted surface, relative to pure error. A large value of $\text{Prob} > F$ for lack of fit is preferred [17]. The lack of fit was insignificantly relevant to the pure error because its p-value was

higher than 0.05, revealing that the model was adequate for the prediction of PHE removal from soil and solution [18, 19].

According to Table 5, UV lamp power, ozone dose, TiO₂ concentration, ethanol fraction, pH, PHE initial concentration, and treatment time were found to be highly significant for PHE removal efficiency. Some developed model parameters were found to be insignificant, such as interaction between time and other independent variables, so these terms have been removed from the model, for increasing the model performance.

The normal probability plot indicates whether the residuals follow a normal distribution, in which case the points will follow a straight line. If there was a definite pattern like an "S-shaped" curve, it means that there is a problem with normality and need for transformation of response [11, 20]. According to Figure 2, the "S- shape" curve was not formed, so there is no need for transformation

of response. The low value of the coefficient of variation (C.V) demonstrates dependability and reproducibility of model; the acceptable of this parameter is in the range of 0.5%_13.5% [21, 22].

The coefficient variation of the developed model in this study was 3.96%, which was in the acceptable range.

Figure 3 illustrates a diagnostic plot between the predicted and actual values. The result confirms that the predicted values are in agreement with the observed ones. It indicates that there was

insignificant violation of the model, and the response surface methodology model is accurate.

According to ANOVA table (Table 5), following was the order of significance for PHE removal efficiency with regard to the F-value: ozone dose (3213.50) > UV power lamp (1269.44) > ethanol fraction (1201.83) > Time (854.37) > TiO₂ concentration (852.84) > pH (187.76) > PHE initial concentration (130.16). These results are also verified by the perturbation plot given in Figure 4.

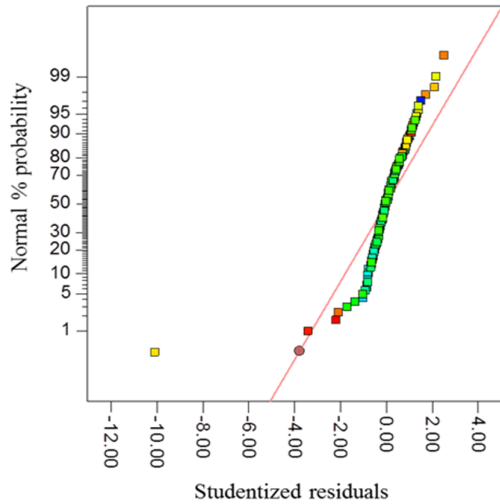


Figure 2. The studentized residual and normal% probability plot of PHE removal efficiency.

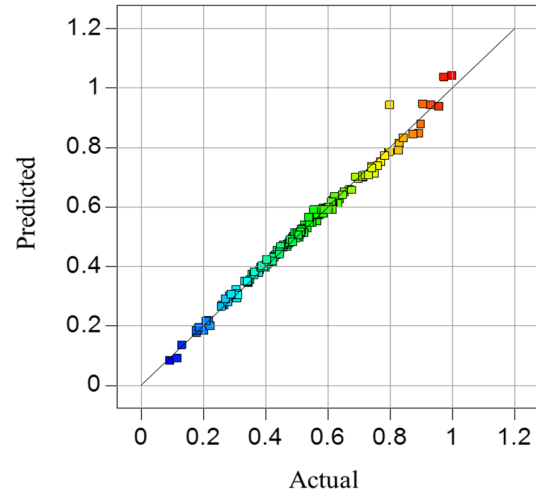


Figure 3. Predicted versus actual data obtained by experimental design by RSM.

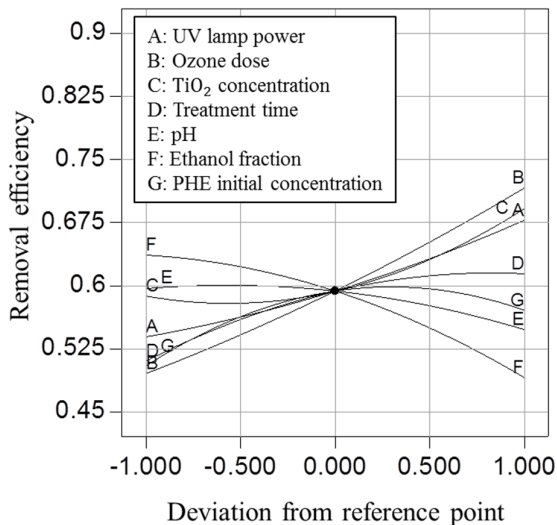


Figure 4. Perturbation plots comparing the effect of all independent variables.

The RSM model equations in terms of actual (uncoded) variables were given in Equation (1); the parameters of this equation are as follow:

UV: UV lamp power (w)

O₃: Ozone dose (mg/L)

TiO₂: TiO₂ concentration (g/m²)

time: Treatment time (min)

pH: pH

ET/W: Ethanol fraction (%)

C_{PHE}: PHE initial concentration (mg/L)

$$\begin{aligned}
 \text{Removal (\%)} = & -0.037042 + 2.06092 \times 10^{-3} \times \text{UV} + 0.33989 \times O_3 - 0.13655 \times \text{TiO}_2 \\
 & + 5.01944 \times 10^{-3} \times \text{time} + 0.015918 \times \text{pH} + 4.38324 \times 10^{-3} \times (\text{ET}/\text{W}) \\
 & + 0.026816 \times C_{\text{PHE}} + 4.21383 \times 10^{-3} \times \text{UV} \times O_3 \\
 & + 7.84415 \times 10^{-4} \times \text{UV} \times \text{TiO}_2 + 7.85784 \times 10^{-5} \times \text{UV} \times \text{pH} \\
 & - 3.59285 \times 10^{-5} \times \text{UV} \times (\text{ET}/\text{W}) - 1.14704 \times 10^{-4} \times \text{UV} \times C_{\text{PHE}} \\
 & + 0.074312 \times O_3 \times \text{TiO}_2 + 7.79534 \times 10^{-4} \times O_3 \times \text{time} \\
 & + 0.011345 \times O_3 \times \text{pH} - 2.72208 \times 10^{-3} \times O_3 \times (\text{ET}/\text{W}) \\
 & - 0.010992 \times O_3 \times C_{\text{PHE}} - 2.96067 \times 10^{-4} \times \text{TiO}_2 \times \text{time} \\
 & + 4.60650 \times 10^{-3} \times \text{TiO}_2 \times \text{pH} - 9.51861 \times 10^{-4} \times \text{TiO}_2 \times (\text{ET}/\text{W}) \\
 & + 3.71080 \times 10^{-5} \times \text{UV}^2 + 0.30441 \times O_3^2 + 0.071804 \times \text{TiO}_2^2 \\
 & - 3.48656 \times 10^{-5} \times \text{time}^2 - 2.38532 \times 10^{-3} \times \text{pH}^2 \\
 & - 3.34176 \times 10^{-5} \times (\text{ET}/\text{W})^2 - 5.58874 \times 10^{-4} \times C_{\text{PHE}}^2
 \end{aligned}
 \tag{1}$$

3.2. Response surface plots

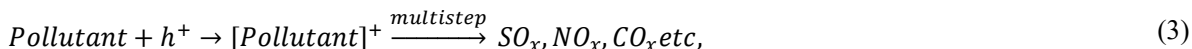
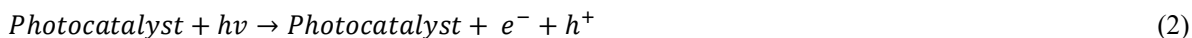
In this section, the distinctive effect of independent variables on PHE removal efficiency, the simultaneous effect of variables, and the interaction between independent variables have been represented.

As described later, UV lamp power, ozone dose, TiO₂ concentration, pH, ethanol fraction, and PHE initial concentration are independent effective variables, and PHE removal efficiency is the dependent variable.

- **Distinctive effect of each variable on removal efficiency**

Figure 5 and Figure 6 show the distinctive effect of independent variables affecting the PHE removal efficiency.

Figure 5(i) shows the positive effect of UV lamp power. According to the figure, by increasing the UV lamp power (from 10 w to 50 w) PHE removal efficiency has been increased (from 53.93% to 67.79%). UV light intensity is increased by increasing the lamp power. According to Equation (2), by increasing the light intensity, electron hole formation predominates, and the rate of hydroxyl radical production is increased, which plays a key role in photocatalytic ozonation processes. Similarly, these results have been proved in other studies, and also according to Equation (3), electron holes can be affective in pollutant mineralization directly.



The effect of ozone dose has been illustrated in Figure 5(ii). According to the figure, by increasing the ozone dose (from 0.1 mg/L to 0.5 mg/L), PHE removal efficiency increased from 49.57% to 71.62%, according to Equations (4)-(6) [23]; water pollutants are presumed to act with ozone, for ozone decomposition to ozonide radical anions and then hydroxyl radical production, which plays a key role for degradation of pollutants in water [24, 25].

Figure 5(iii) shows that by increasing the TiO₂ concentration (from 0.5 g/m² to 2.1 g/m²), PHE removal efficiency increased from 58.79% to

69.16%. Good adsorption and interaction between pollutant molecule are required in photocatalytic processes. According to other studies, TiO₂ can adsorb soluble PHE, so by increasing the TiO₂ concentration, the rate of PHE adsorption increased [26]. Also, electron hole generation was increased by increasing the TiO₂ concentration, so according to Equation (3), the pollutant mineralization ability was increased.

Figure 5(iv) shows that by increasing the time, PHE removal efficiency is increased. The higher contacts between the produced radicals and the contaminant particles have led to this situation.

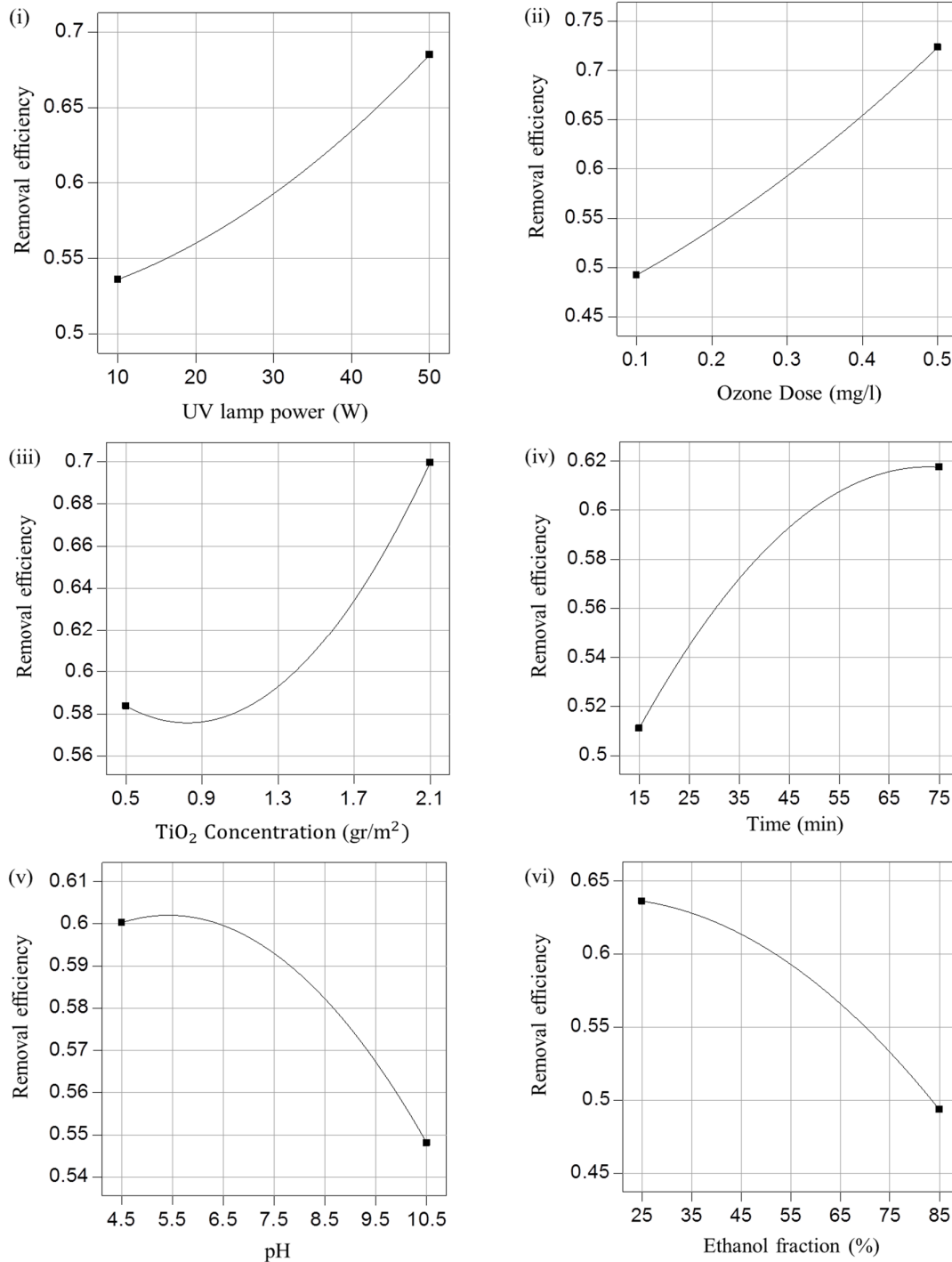


Figure 5. Direct effect of independent variables on PHE removal efficiency. (i) UV lamp power (w) (ozone dose = 0.35 mg/L, TiO₂ concentration = 1.3 g/m², time = 45 min, pH = 7.5, ethanol fraction = 55%, PHE concentration = 15mg/L), (ii) ozone dose (mg/L) (UV lamp power = 30 w, TiO₂ concentration = 1.3 g/m², time = 45 min, pH = 7.5, ethanol fraction = 55%, PHE concentration = 15mg/L), (iii) TiO₂ concentration (g/m²) (UV lamp power = 30 w, ozone dose = 0.35 mg/L, time = 45 min, pH = 7.5, ethanol fraction = 55%, PHE concentration = 15mg/L), (iv) time (min) (UV lamp power = 30 w, ozone dose = 0.35 mg/L, TiO₂ concentration = 1.3 g/m², pH = 7.5, ethanol fraction = 55%, PHE concentration = 15mg/L), (v) pH (UV lamp power = 30w, Ozone dose = 0.35 mg/L, TiO₂ concentration = 1.3 g/m², time = 45 min, ethanol fraction = 55%, PHE concentration = 15mg/L), (vi) ethanol fraction (%) (UV lamp power = 30 w, ozone dose = 0.35 mg/L, TiO₂ concentration = 1.3 g/m², time = 45 min, PHE concentration = 15mg/L).

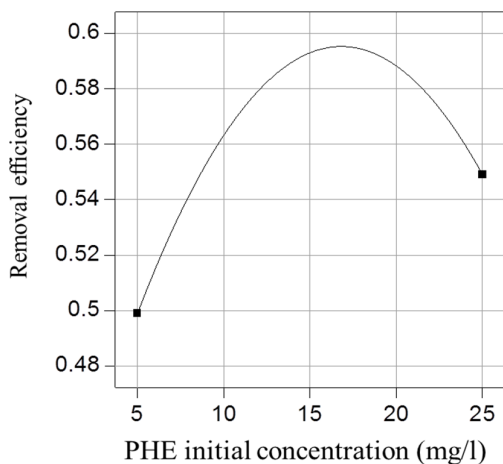
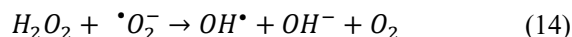
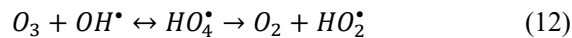
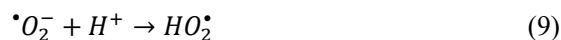
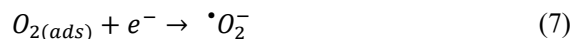


Figure 6. Direct effect of PHE concentration on removal efficiency (mg/L), (UV lamp power = 30 (w), ozone dose = 0.35 mg/L, TiO₂ concentration = 1.3 g/m², time = 45 min, pH = 7.5, ethanol fraction = 55%).

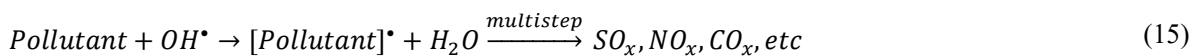


The effect of pH has been investigated in Figure 5(v). According to this figure, by increasing the pH from 4.5 to 5.6, the PHE removal efficiency increased from 59% to 61%, and by increasing the pH from 5.6 to 10.5, the PHE removal efficiency decreased from 62% to 54%. According to Equation **Error! Reference source not found.**, UV radiation can provide the appropriate band gap energy to generate photo-activated electron-hole pairs, and as shown in equations (7) and (8), the photo-generated electrons (e^-) react with adsorbed oxygen and adsorbed ozone molecules as electron

acceptors [27, 28]. Ozonide radical anions and superoxide ($\cdot O_3^-$ and $\cdot O_2^-$), which are reactive intermediates in the photocatalytic ozonation process, react with H^+ , and then HO_2^\bullet and HO_3^\bullet were produced (Equation (9) and (10)) [23]. According to Equation (11), for hydroxyl radical production, the ozonide radicals should react with H^+ , so by increasing the amount of H^+ , hydroxyl radical production was increased. According to Equations (12) and (13), H_2O_2 is an intermediate production of Equation (11) reaction, which as shown, H^+ has a key role for this production. According to Equation (14), hydrogen peroxide molecules can also react with $\cdot O_2^-$, and produce the hydroxyl radical. As shown, H^+ is the initiator factor for these processes.



Hydroxyl radicals produced in the aforementioned processes (Equations **Error! Reference source not found.**-(14)) attack target pollutant molecules and decompose them to less harmful substance (Equation (15)) [23].



Other published studies indicated acidic pH being preferred for photocatalytic ozonation processes [29, 30]. Furthermore, according to other studies at pH 7, accumulated bicarbonate ions can scavenge the hydroxyl radical produced and reduction of the oxidation efficiency [31]. In addition, it was observed that in the presence of the TiO₂ as the catalyst, the generation of the hydroxyl radicals takes place at pH 5 [31]. Thus, as shown in Figure 5(v), pH 5 is the best pH for photocatalytic ozonation processes.

Figure 5(vi) shows the negative effect of ethanol fraction on the PHE removal efficiency. This removal efficiency decrease is due to ethanol ability to consume of $\cdot OH$. Thus by increasing the ethanol fraction (from 25% to 85%) the removal efficiency is decreased (from 62% to 52%), which have been confirmed in other similar studies (Lundstedt, Persson, & Öberg, 2006).

Figure 6 shows the effect of PHE initial concentration. According to the figure, by increasing the PHE initial concentration (from 5

mg/L to 17.67 mg/L), the removal efficiency increased from 50.48% to 59.87%. This improvement is due to increased availability of pollutant for oxidative reaction with active oxidising species. This is also true in other similar studies [32, 33].

▪ Simultaneous effect of variables on removal efficiency

Three-dimensional surface was obtained to demonstrate the different relationship between the dependent and independent variables.

Figure 7(i) is plotted to study the simultaneous effect of UV lamp power and ozone dose. According to the figure, by increasing the UV lamp power (from 10 w to 50 w) and ozone dose (from 0.1 mg/L to 0.5 mg/L), the PHE removal efficiency increased from 45% to 80%. This significant improvement is due to increased hydroxyl radical production. As described in Figure 5(i) and (ii), by increasing either UV lamp power or ozone dose, hydroxyl radical production increased; thus, by increasing both UV lamp power and ozone dose, the rate of hydroxyl radical production increased, and there is a significant PHE removal efficiency improvement. Also, this figure shows that the ozone dose is more effective than UV lamp power; it is associated with ozone participation in several reactions, which lead to hydroxyl radical production [3, 34].

The simultaneous effect of TiO₂ concentration and UV lamp power has been investigated in Figure 7(ii). According to this figure, the maximum PHE removal efficiency has been occurred at maximum UV lamp power and maximum TiO₂ concentration. As clear at minimum value of UV lamp power, there is a mild PHE removal efficiency improvement, by TiO₂ concentration increasing; in this condition, PHE adsorption by TiO₂ is a predominant process, so by increasing the TiO₂ concentration, just PHE adsorption rate is increased, and there is not enough hydroxyl radical, so a mild PHE removal efficiency improvement has been observed.

Figure 7(iii) shows the simultaneous effect between pH and UV lamp power. According to this

figure, maximum PHE removal efficiency has been achieved in the maximum UV lamp power and the minimum pH; in this condition, there are enough H⁺ cation and electron-hole pairs for hydroxyl radical production. As shown, PHE removal efficiency improvement slope at a constant pH is higher than it at a constant UV lamp power, which shows that the UV lamp power is the predominated variable.

The simultaneous effect of ethanol fraction and UV lamp power is illustrated in Figure 7(iv).

According to the figure, at the maximum value of ethanol fraction and minimum UV lamp power, the minimum PHE removal efficiency is observed; at this situation, electron-hole pairs, which have a key role in hydroxyl radical production, there are at the minimum value of whose, and in presence of ethanol, this produced radical hydroxyl is consumed by ethanol [35].

Thus, at the maximum level of UV lamp power and minimum value of ethanol fraction, the rate of hydroxyl radical production increased, and the rate of consumption them decreased, so in this situation, the maximum PHE removal efficiency is occurred. This is true in other similar studies [1].

Figure 7(v) shows the simultaneous effect of UV lamp power and PHE initial concentration. According to the figure, the maximum PHE removal efficiency has been occurred at UV lamp power of 50 w and 17.67 mg/L PHE initial concentration. As described at Figure 6, by increasing the PHE initial concentration (from 5 mg/L to 17.67 mg/L), the availability of pollutant for oxidative reactions is increased [32, 33]. Also, the rate of hydroxyl radical production is increased by increasing the UV lamp power. According to Figure 7(vi), at the maximum level of TiO₂ concentration and ozone dose (at UV lamp power = 30 w, ethanol fraction = 55%, time = 45 min, pH = 7.5, PHE concentration = 15 mg/L), the maximum PHE removal efficiency has been achieved. Increasing the ozone dose leads to produce more hydroxyl radicals [24, 25]. Also increasing the TiO₂ concentration leads to increase PHE adsorption [26]. Thus, by simultaneous increasing of ozone dose and TiO₂ concentration, the PHE removal efficiency is improved.

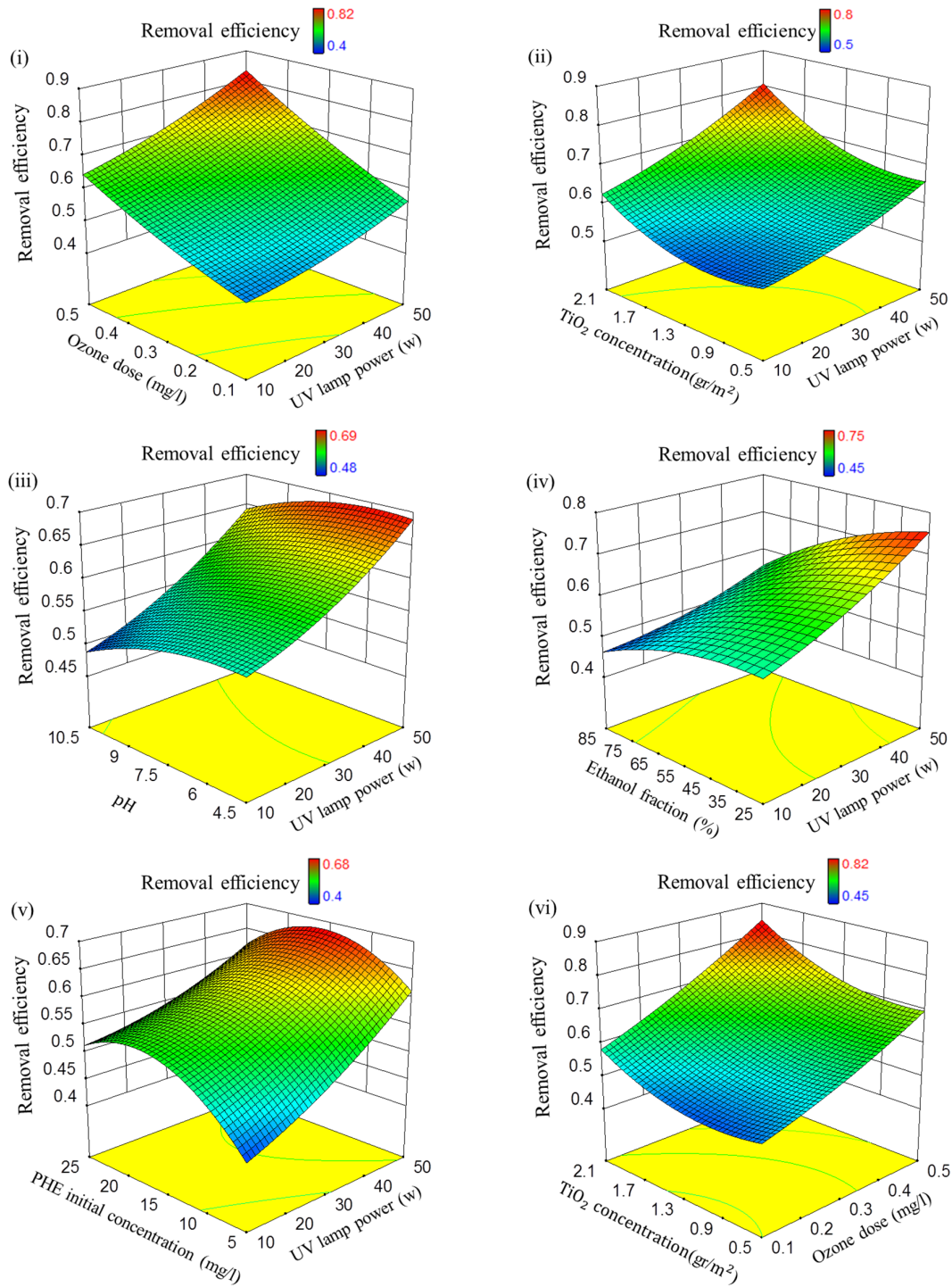


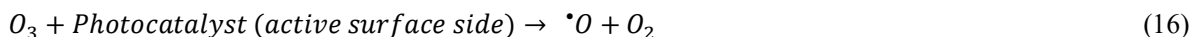
Figure 7. Three-dimensional surface for PHE removal efficiency. (i) UV lamp power (w) and ozone dose (mg/l) (TiO₂ concentration = 1.3 g/m², time = 45 min, pH = 7.5, ethanol fraction = 55%, PHE concentration = 15 mg/L), (ii) UV lamp power (w) and TiO₂ concentration (g/m²) (ozone dose = 0.35 mg/L, time = 45 min, pH = 7.5, ethanol fraction = 55%, PHE concentration = 15 mg/L), (iii) UV lamp power (w) and pH (ozone dose = 0.35 mg/L, TiO₂ concentration = 1.3 g/m², time = 45 min, ethanol fraction = 55%, PHE concentration = 15 mg/L), (iv) UV lamp power (w) and ethanol fraction (%) (ozone dose = 0.35 mg/L, TiO₂ concentration = 1.3 g/m², pH = 7.5, PHE concentration = 15 mg/L), (v) UV lamp power (w) and PHE initial concentration (mg/l) (Ozone dose = 0.35 mg/L, TiO₂ concentration = 1.3 g/m², time = 45 min, ethanol fraction = 55%, pH = 7.5), (vi) ozone dose (mg/L) and TiO₂ concentration (g/m²) (UV lamp power = 30 w, ethanol fraction = 55%, time = 45 min, pH = 7.5, PHE concentration = 15 mg/L).

▪ **Interaction between variables affecting PHE removal efficiency**

The interaction between independent variables has been plotted in ten modes in Figure 8 and Figure 9. Removal efficiency changes are plotted against continual changes of a variable and at the high level and low level of the other one. If the removal efficiency changes slope changed, there is a significant interaction between tow parameters (synergetic or antagonistic); otherwise, each two have neutral effect on each other [36].

Figure 8(i) shows the interaction between UV lamp power and ozone dose. According to the

figure, PHE removal efficiency is increased by increasing UV lamp power, and the slope of this increasing at ozone dose of 0.5 mg/L is more than ozone dose of 0.1 mg/L; in other words, increasing the ozone dose level, increased the slope of PHE removal efficiency enhancement. Thus there is a synergetic interaction between UV lamp power and ozone dose. According to Equations (16)-(18) [23], photocatalyst improved the ozone ability for hydroxyl radical production. The synergetic interaction between ozone dose and UV lamp power has been proved in similar studies [37, 38].



The interaction between UV lamp power and TiO₂ concentration has been investigated in Figure 8(ii). According to this figure, at TiO₂ concentration of 0.5 g/m², by increasing the UV lamp power (from 10 w to 50 w), the PHE removal efficiency increased from 54.60% to 65.94%, and at TiO₂ concentration of 2.1 g/m², by increasing the UV lamp power (from 10 w to 50 w), the PHE removal efficiency increased from 62.46% to 78.83%. As clear, by increasing the TiO₂ concentration (from 0.5 g/m² to 2.1 g/m²), the slope of PHE removal efficiency improvement increased. Thus, there is a synergetic effect between UV lamp power and TiO₂ concentration. According to Equation (3) and other similar studies [8], this result is proved.

Figure 8(iii) has illustrated the interaction between UV lamp power and pH; according to this figure, there is a synergetic effect between this independent variable. As shown in Equation (19), OH⁻ reacts with h⁺ (positive electron hole) and produces the hydroxyl radical. Thus, alkalinity pH can improve the UV lamp performance [39, 40], but because of ozone presence, acidic pH is better for photocatalytic ozonation processes.



Figure 8(iv) shows the interaction between UV lamp power and ethanol fraction. According to the figure, ethanol fraction increase decreased the slope of PHE removal efficiency enhancement.

Thus, there is an antagonistic interaction between this independent variable. Ethanol covered the surface of TiO₂, so the UV lamp performance decreased; it is true according to similar studies [1].

According to Figure 8(v), there is an antagonistic interaction between UV lamp power and PHE initial concentration. As shown, the slope of PHE removal efficiency improvement is decreased by increasing the PHE initial concentration. Similar studies have proved this result [26]. According to Equation (3), by increasing the pollutant concentration, the rate of h⁺ consumption is increased. But in the presence of ozone, increasing of PHE initial concentration lead to removal efficiency improvement [32, 33].

The interaction between ozone dose and TiO₂ concentration has been investigated in Figure 8(vi). According to this figure, at TiO₂ concentration of 0.5 g/m², by increasing the ozone dose (from 0.1 mg/L to 0.5 mg/L), the PHE removal efficiency increased from 50.17% to 67.84%, and at TiO₂ concentration of 2.1 g/m², by increasing the ozone dose, the PHE removal efficiency increased from 58.17% to 82.59%. On the other hand, in the range of ozone changes, at TiO₂ concentration of 0.5 g/m² and 2.1 g/m², PHE removal efficiency increased 17.67% and 24.32%, respectively. Thus there is a synergetic interaction between ozone dose and TiO₂ concentration. According Equation (16), it is true, because by increasing the TiO₂ concentration, the photocatalyst active surface sites, which react with ozone increased, so the rate of oxygen atom radical and hydroxyl radical production increased.

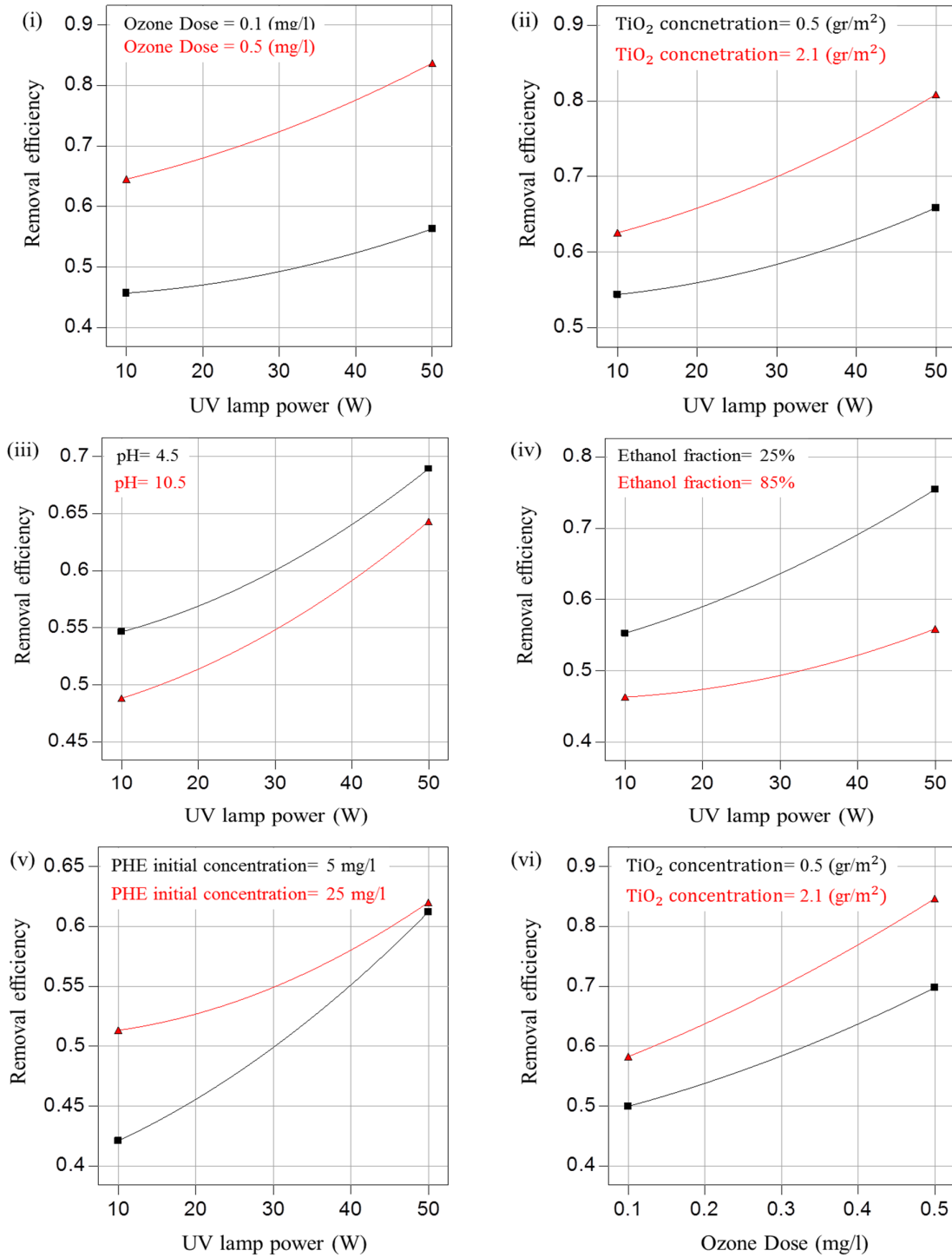


Figure 8. Interaction plot for: (i) UV lamp power (w) and ozone dose (mg/L) (TiO₂ concentration =1.3 g/m², time = 45 min, pH =7.5, ethanol fraction = 55%, PHE concentration = 15 mg/L), (ii) UV lamp power (w) and TiO₂ concentration (g/m²) (ozone dose = 0.35 mg/L, time = 45 min, pH = 7.5, ethanol fraction = 55%, PHE concentration = 15 mg/L), (iii) UV lamp power (w) and pH (ozone dose = 0.35 mg/l, TiO₂ concentration = 1.3 g/m², time = 45 min, ethanol fraction = 55%, PHE concentration = 15 mg/L), (iv) UV lamp power (w) and ethanol fraction (%) (ozone dose = 0.35 mg/L, TiO₂ concentration = 1.3 g/m², pH = 7.5, PHE concentration = 15 mg/L), (v) UV lamp power (w) and PHE initial concentration (mg/L) (ozone dose = 0.35 mg/L, TiO₂ concentration = 1.3 g/m², time = 45 min, ethanol fraction = 55%, pH = 7.5), (vi) ozone dose (mg/L) and TiO₂ concentration (g/m²) (UV lamp power = 30 w, ethanol fraction = 55%, time = 45 min, pH = 7.5, PHE concentration = 15mg/L).

The synergetic interaction between ozone dose and pH has been illustrated in Figure 9(i). According to this figure, by increasing the pH, the PHE removal efficiency slope, increased, so there is a synergetic interaction between these independent variables. As shown in Equation (20), ozone molecules react with OH^- and produce $\cdot O_2^-$ and $HO_2\cdot$ which are as initiators for hydroxyl radical production. This is also true in other similar studies [7].



Figure 9(ii) shows the interaction between ozone dose and ethanol fraction. According to this figure, there is an antagonistic interaction between ozone dose and ethanol fraction. By increasing the amount of ethanol, TiO_2 active surface sites covered by ethanol, and the rate of oxygen atom radical production decreases, which is an initiator for hydroxyl radical production, so the ozone performance is decreased by increasing the ethanol fraction; these results are concluded in similar studies [1].

The antagonistic interaction between ozone dose and PHE initial concentration has been illustrated in Figure 9(iii). According to Equation (21) [23], ozone is consumed by increasing the PHE initial concentration, so ozone molecules cannot participate in other reactions that lead to hydroxyl radical production. This is also true in other similar studies [23].



The interaction between ethanol fraction and TiO_2 concentration has been investigated in Figure 9(iv). As clear, there is an antagonistic interaction between ethanol fraction and TiO_2 concentration. Ethanol covered the TiO_2 surface, and decrease the TiO_2 ability for PHE adsorption and the potential of hydroxyl radical production; Thus the TiO_2 performance is decreased by increasing the ethanol fraction. Similarly, these results have been proved in other studies [2].

3.3. Optimization

The main of RSM is to establish an empirical formula, and also optimizing the objective function according to its variables and its boundary conditions. In this study, Equation (1) is the objective UV lamp power, ozone dose, TiO_2 concentration, ethanol fraction, treatment time, pH, and initial PHE concentration are the optimization variables; the purpose of optimization is to achieve to maximum PHE removal efficiency. The boundary condition of each variable is represented in Table 6.

Figure 10 and Figure 11 show the optimization results of PHE removal efficiency objective function. According to these figures, at 47.242 w UV lamp power, ozone dose of 0.499 mg/L, 2.092 g/m² TiO_2 concentration, in 41.664 min, pH = 5.282, ethanol fraction of 25% and 14.64 mg/L initial PHE concentration, the maximum PHE removal efficiency is achieved that is equal to 100%, theoretically.

Table 2. Variable boundary conditions for optimization.

Parameters	Lower limit	Upper limit
UV lamp power (w)	10	50
Ozone dose (mg/L)	0.1	0.5
TiO_2 concentration (g/m ²)	0.5	2.1
Ethanol fraction (%)	25	85
pH	4.5	10.5
Initial PHE concentration (mg/L)	5	25
Treatment time (min)	15	45

For validation of optimization results, the physical model was run at UV lamp power of 40 w, ethanol fraction of 25%, and 15 mg/L PHE concentration; the ozone dose was 0.5 mg/L in the pH of 5.2, TiO_2 concentration of 2 g/m²; and during

40 min treatment, the experimental result shows that the PHE removal efficiency at this condition is about 98%. This difference is due to operator and equipment errors. Other studies were achieved to 80%-90% PAHs removal efficiency [1, 41, 42, 43].

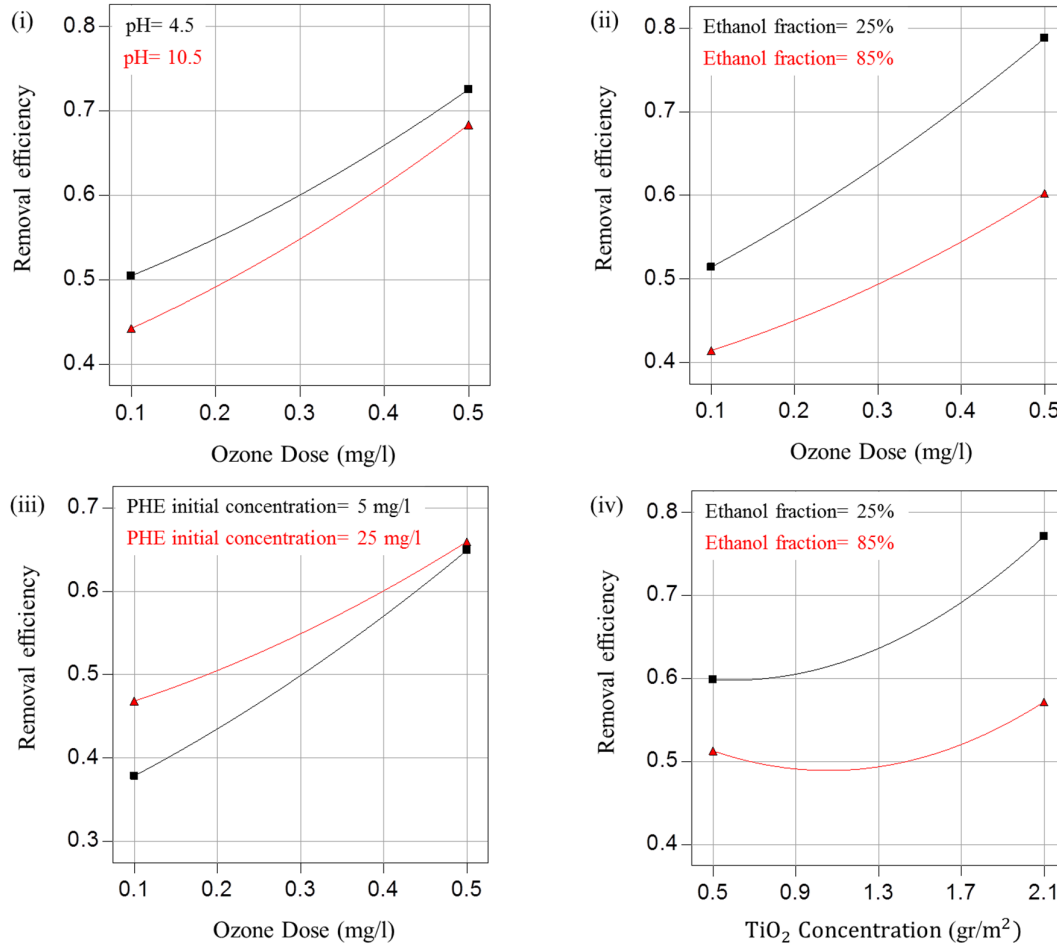


Figure 9. Interaction plot for: (i) pH and ozone dose (mg/L) (UV lamp power = 55 w, TiO₂ concentration = 1.3 g/m², time = 45 min, ethanol fraction = 55%, PHE concentration = 15mg/L), (ii) ozone dose (mg/L) and ethanol fraction (%) (UV lamp power = 55 w, TiO₂ concentration = 1.3 g/m², time = 45 min, pH = 7.5, PHE concentration = 15 mg/L), (iii) ozone dose (mg/L) and PHE initial concentration (mg/L) (UV lamp power = 55 w, TiO₂ concentration = 1.3 g/m², time = 45 min, ethanol fraction = 55%, pH = 7.5), (iv) TiO₂ concentration (g/m²) and ethanol fraction (%) (UV lamp power = 55 w, ozone dose = 0.35 mg/L, pH = 7.5, PHE concentration = 15 mg/L).

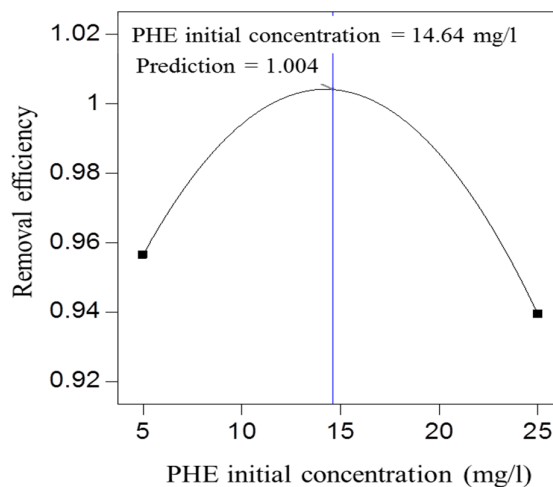


Figure 10. Optimum value of PHE initial concentration (UV lamp power = 47.242 w, ozone dose = 0.499 mg/L, TiO₂ concentration = 2.099 g/m², time = 41.664 min, ethanol fraction = 25%).

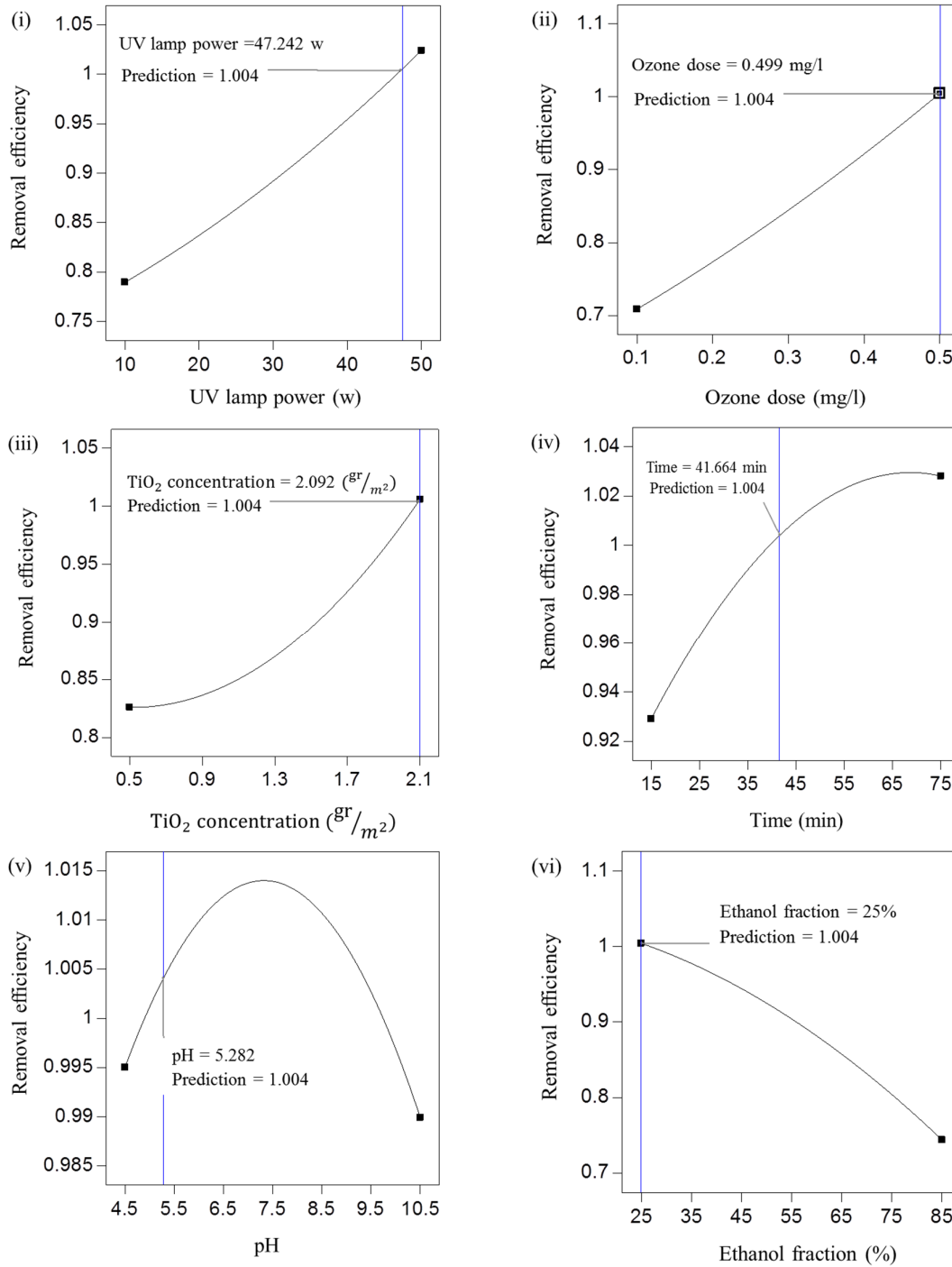


Figure 11. Optimum value of each independent variable: (i) UV lamp power (w) (ozone dose = 0.499 mg/L, TiO₂ concentration = 2.092 g/m², time = 41.664 min, pH = 5.282, ethanol fraction = 25%, PHE concentration = 14.64 mg/L), (ii) Ozone dose (mg/L) (UV lamp power = 47.242w, TiO₂ concentration = 2.092 gr/m², time = 41.664 min, pH = 5.282, ethanol fraction = 25%, PHE concentration = 14.64 mg/L), (iii) TiO₂ concentration (g/m²) (UV lamp power = 47.242 w, ozone dose = 0.499 mg/L, time = 41.664 min, pH = 5.282, ethanol fraction = 25%, PHE concentration = 14.64 mg/L), (iv) time (min) (UV lamp power = 47.242 w, Ozone dose = 0.499 mg/L, TiO₂ concentration = 2.092 g/m², pH = 5.282, ethanol fraction = 25%, PHE concentration = 14.64 mg/L), (v) pH (UV lamp power = 47.242 w, ozone dose = 0.499 mg/L, TiO₂ concentration = 2.099 g/m², time = 41.664 min, ethanol fraction = 25%, PHE concentration = 14.64 mg/L), (vi) Ethanol fraction (%) (UV lamp power = 47.242w, Ozone dose = 0.499 mg/l, TiO₂ concentration = 2.099 g/m², time = 41.664 min, PHE concentration = 14.64 mg/L).

4. Conclusions

In conclusion, this study demonstrates a novel and effective approach for the removal of polycyclic aromatic hydrocarbons (PAHs) from soil washing solutions. By harnessing the simultaneous application of ozone and the photocatalytic activity of TiO₂ nanoparticles under UV irradiation, we have achieved a favorable performance in the degradation of PAHs. The significance of this research work lies in its unique contribution to the field, offering a practical and efficient solution to the persistent challenge of PAH contamination. The synergistic effects of ozone and TiO₂ photocatalysis provide a promising avenue for environmental remediation, showcasing the potential for a sustainable and advanced treatment method. Moreover, the application of response surface methodology (RSM) in modeling this intricate process enhances our understanding of the complex interplay between various parameters. Through systematic optimization, we have identified key operational conditions that maximize the efficiency of PAH removal. The optimized values including UV lamp power, ozone dose, TiO₂ concentration, ethanol fraction, pH, initial PAH concentration, and treatment time (40 W, 0.5 mg/L, 2 g/m², 25%, 5.2, 15 mg/L, 40 min, respectively), serve as practical guidelines for the implementation of this innovative approach. The overarching novelty of our research work lies not only in the efficacy of the combined ozone and TiO₂ photocatalysis but also in the systematic optimization facilitated by RSM. This study advances our understanding of pollutant removal processes, and offers a blueprint for the application of this environmentally friendly and economically viable method.

References

- [1]. Aguilar, C. M., Rodríguez, J. L., Chairez, I., Tiznado, H., & Poznyak, T. (2017). Naphthalene degradation by catalytic ozonation based on nickel oxide: study of the ethanol as cosolvent. *Environmental Science and Pollution Research*, 24(33), 25550–25560. <https://doi.org/10.1007/s11356-016-6134-2>
- [2]. Aguilar, C. M., Rodríguez, J. L., Chairez, I., Tiznado, H., & Poznyak, T. (2016). Naphthalene degradation by catalytic ozonation based on nickel oxide: study of the ethanol as cosolvent. *Environmental Science and Pollution Research* 2016 24:33, 24(33), 25550–25560. <https://doi.org/10.1007/S11356-016-6134-2>
- [3]. Li, L., Zhang, P., Zhu, W., Han, W., & Zhang, Z. (2005). Comparison of O₃-BAC, UV/O₃-BAC and TiO₂/UV/O₃-BAC processes for removing organic pollutants in secondary effluents. *Journal of Photochemistry and Photobiology A: Chemistry*, 171(2), 145–151. <https://doi.org/10.1016/J.JPHOTOCHEM.2004.09.016>
- [4]. Li, H., Gong, Y., Huang, Q., & Zhang, H. (2013). Degradation of orange II by UV-assisted advanced fenton process: Response surface approach, degradation pathway, and biodegradability. *Industrial and Engineering Chemistry Research*, 52(44), 15560–15567. <https://doi.org/10.1021/IE401503U>
- [5]. Wang, Z., Zheng, X., Wang, Y., Lin, H., & Zhang, H. (2021). Evaluation of phenanthrene removal from soil washing effluent by activated carbon adsorption using response surface methodology. *Chinese Journal of Chemical Engineering*. <https://doi.org/10.1016/J.CJCHE.2021.02.027>
- [6]. Yap, C. L., Gan, S., & Ng, H. K. (2012). Ethyl lactate-Fenton treatment of soil highly contaminated with polycyclic aromatic hydrocarbons (PAHs). *Chemical Engineering Journal*, 200–202, 247–256. <https://doi.org/10.1016/j.cej.2012.06.036>
- [7]. Luster-Teasley, S., Ubaka-Blackmoore, N., & Masten, S. J. (2009). Evaluation of soil pH and moisture content on in-situ ozonation of pyrene in soils. *Journal of Hazardous Materials*, 167(1–3), 701–706. <https://doi.org/10.1016/j.jhazmat.2009.01.046>
- [8]. Uv, O., Uv, T., Uv, O. T., Pengyi, Z., Fuyan, L., Gang, Y., Qing, C., & Wanpeng, Z. (2003). A comparative study on decomposition of gaseous toluene, 156, 189–194. [https://doi.org/10.1016/S1010-6030\(02\)00432-X](https://doi.org/10.1016/S1010-6030(02)00432-X)
- [9]. Im, J. K., Cho, I. H., Kim, S. K., & Zoh, K. D. (2012). Optimization of carbamazepine removal in O₃/UV/H₂O₂ system using a response surface methodology with central composite design. *Desalination*, 285, 306–314. <https://doi.org/10.1016/J.DESAL.2011.10.018>
- [10]. Körbahti, B. K., & Rauf, M. A. (2008). Response surface methodology (RSM) analysis of photoinduced decoloration of toluidine blue. *Chemical Engineering Journal*, 136(1), 25–30. <https://doi.org/10.1016/J.CEJ.2007.03.007>
- [11]. Wu, J., Zhang, H., Oturan, N., Wang, Y., Chen, L., & Oturan, M. A. (2012). Application of response surface methodology to the removal of the antibiotic tetracycline by electrochemical process using carbon-felt cathode and DSA (Ti/RuO₂-IrO₂) anode. *Chemosphere*, 87(6), 614–620. <https://doi.org/10.1016/J.CHEMOSPHERE.2012.01.036>
- [12]. Buthiyappan, A., Raja Ehsan Shah, R. S. S., Asghar, A., Abdul Raman, A. A., Daud, M. A. W., Ibrahim, S., & Tezel, F. H. (2019). Textile wastewater treatment efficiency by Fenton oxidation with integration of membrane separation system. *Chemical*

- Engineering Communications*, 206(4), 541–557. <https://doi.org/10.1080/00986445.2018.1508021>
- [13]. Khataee, A. R., Fathinia, M., Aber, S., & Zarei, M. (2010). Optimization of photocatalytic treatment of dye solution on supported TiO₂ nanoparticles by central composite design: Intermediates identification. *Journal of Hazardous Materials*, 181(1–3), 886–897. <https://doi.org/10.1016/J.JHAZMAT.2010.05.096>
- [14]. Arslan-Alaton, I., Ayten, N., & Olmez-Hanci, T. (2010). Photo-Fenton-like treatment of the commercially important H-acid: Process optimization by factorial design and effects of photocatalytic treatment on activated sludge inhibition. *Applied Catalysis B: Environmental*, 96(1–2), 208–217. <https://doi.org/10.1016/J.APCATB.2010.02.023>
- [15]. Körbahti, B. K. (2007). Response surface optimization of electrochemical treatment of textile dye wastewater. *Journal of Hazardous Materials*, 145(1–2), 277–286. <https://doi.org/10.1016/J.JHAZMAT.2006.11.031>
- [16]. Borror, C. M., Montgomery, D. C., & Myers, R. H. (2018). Evaluation of Statistical Designs for Experiments Involving Noise Variables. *Https://Doi.Org/10.1080/00224065.2002.11980129*, 34(1), 54–70. <https://doi.org/10.1080/00224065.2002.11980129>
- [17]. Zainal-Abideen, M., Aris, A., Yusof, F., Abdul-Majid, Z., Selamat, A., & Omar, S. I. (2012). Optimizing the coagulation process in a drinking water treatment plant – comparison between traditional and statistical experimental design jar tests. *Water Science and Technology*, 65(3), 496–503. <https://doi.org/10.2166/WST.2012.561>
- [18]. Buthiyappan, A., Shah, R. S. S. R. E., Asghar, A., Raman, A. A. A., Daud, M. A. W., Ibrahim, S., & Tezel, F. H. (2018). Textile wastewater treatment efficiency by Fenton oxidation with integration of membrane separation system. *Https://Doi.Org/10.1080/00986445.2018.1508021*, 206(4), 541–557. <https://doi.org/10.1080/00986445.2018.1508021>
- [19]. Bezerra, M. A., Santelli, R. E., Oliveira, E. P., Villar, L. S., & Escalera, L. A. (2008, September 15). Response surface methodology (RSM) as a tool for optimization in analytical chemistry. *Talanta*. Elsevier. <https://doi.org/10.1016/j.talanta.2008.05.019>
- [20]. Khuri, A. I. (2006). Response surface methodology and related topics, 457.
- [21]. Ahmad, A. L., Ismail, S., & Bhatia, S. (2005). Optimization of coagulation-flocculation process for palm oil mill effluent using response surface methodology. *Environmental Science and Technology*, 39(8), 2828–2834. https://doi.org/10.1021/ES0498080/SUPPL_FILE/ES0498080SI20050118_034454.PDF
- [22]. Yetilmezsoy, K., Demirel, S., & Vanderbei, R. J. (2009). Response surface modeling of Pb(II) removal from aqueous solution by Pistacia vera L.: Box–Behnken experimental design. *Journal of Hazardous Materials*, 171(1–3), 551–562. <https://doi.org/10.1016/J.JHAZMAT.2009.06.035>
- [23]. Mehrjouei, M., Müller, S., & Möller, D. (2015). A review on photocatalytic ozonation used for the treatment of water and wastewater. *Chemical Engineering Journal*, 263, 209–219. <https://doi.org/10.1016/j.cej.2014.10.112>
- [24]. Beltrán, F. J., Aguinaco, A., Rey, A., & García-Araya, J. F. (2012). Kinetic studies on black light photocatalytic ozonation of diclofenac and sulfamethoxazole in water. *Industrial and Engineering Chemistry Research*, 51(12), 4533–4544. https://doi.org/10.1021/IE202525F/SUPPL_FILE/IE202525F_SI_001.PDF
- [25]. Sein, M. M., Zedda, M., Tuerk, J., Schmidt, T. C., Golloch, A., & Von Sonntag, C. (2008). Oxidation of diclofenac with ozone in aqueous solution. *Environmental Science and Technology*, 42(17), 6656–6662. https://doi.org/10.1021/ES8008612/SUPPL_FILE/ES8008612_FILE001.PDF
- [26]. Zhang, Y., Wong, J. W. C., Liu, P., & Yuan, M. (2011). Heterogeneous photocatalytic degradation of phenanthrene in surfactant solution containing TiO₂ particles. *Journal of Hazardous Materials*, 191(1–3), 136–143. <https://doi.org/10.1016/j.jhazmat.2011.04.059>
- [27]. Augugliaro, V., Litter, M., Palmisano, L., & Soria, J. (2006). The combination of heterogeneous photocatalysis with chemical and physical operations: A tool for improving the photoprocess performance. *Journal of Photochemistry and Photobiology C: Photochemistry Reviews*, 7(4), 127–144. <https://doi.org/10.1016/J.JPHOTOCHEMREV.2006.12.001>
- [28]. Rivas, F. J., Beltrán, F. J., Gimeno, O., & Carbajo, M. (2005). Fluorene Oxidation by Coupling of Ozone, Radiation, and Semiconductors: A Mathematical Approach to the Kinetics. *Industrial and Engineering Chemistry Research*, 45(1), 166–174. <https://doi.org/10.1021/IE050781I>
- [29]. Beltrán, F. J., Rivas, F. J., Gimeno, O., & Carbajo, M. (2005). Photocatalytic Enhanced Oxidation of Fluorene in Water with Ozone. Comparison with Other Chemical Oxidation Methods. *Industrial and Engineering Chemistry Research*, 44(10), 3419–3425. <https://doi.org/10.1021/IE048800W>
- [30]. Yildirim, A. Ö., Gül, Ş., Eren, O., & Kuşvuran, E. (2011). A Comparative Study of Ozonation, Homogeneous Catalytic Ozonation, and Photocatalytic Ozonation for C.I. Reactive Red 194 Azo Dye Degradation. *CLEAN – Soil, Air, Water*, 39(8), 795–805.

<https://doi.org/10.1002/CLEN.201000192>

- [31]. García-Araya, J. F., Beltrán, F. J., & Aguinaco, A. (2010). Diclofenac removal from water by ozone and photolytic TiO₂ catalysed processes. *Journal of Chemical Technology & Biotechnology*, 85(6), 798–804. <https://doi.org/10.1002/JCTB.2363>
- [32]. Beltrán, F. J., Aguinaco, A., Rey, A., & García-Araya, J. F. (2012b). Kinetic studies on black light photocatalytic ozonation of diclofenac and sulfamethoxazole in water. *Industrial and Engineering Chemistry Research*, 51(12), 4533–4544. https://doi.org/10.1021/IE202525F/SUPPL_FILE/IE202525F_SI_001.PDF
- [33]. Rey, A., Quiñones, D. H., Álvarez, P. M., Beltrán, F. J., & Plucinski, P. K. (2012). Simulated solar-light assisted photocatalytic ozonation of metoprolol over titania-coated magnetic activated carbon. *Applied Catalysis B: Environmental*, 111–112, 246–253. <https://doi.org/10.1016/J.APCATB.2011.10.005>
- [34]. Černigoj, U., Štangar, U. L., & Trebše, P. (2007). Degradation of neonicotinoid insecticides by different advanced oxidation processes and studying the effect of ozone on TiO₂ photocatalysis. *Applied Catalysis B: Environmental*, 75(3–4), 229–238. <https://doi.org/10.1016/J.APCATB.2007.04.014>
- [35]. Lundstedt, S., Persson, Y., & Öberg, L. (2006). Transformation of PAHs during ethanol-Fenton treatment of an aged gasworks' soil. *Chemosphere*, 65(8), 1288–1294. <https://doi.org/10.1016/J.CHEMOSPHERE.2006.04.031>
- [36]. Tamadoni, A., & Qaderi, F. (2020). Environmental-economical assessment of the use of ultrasonication for pre-treatment of the soils contaminated by phenanthrene. *Journal of Environmental Management*, 259, 109991. <https://doi.org/10.1016/j.jenvman.2019.109991>
- [37]. Ochiai, T., Nanba, H., Nakagawa, T., Masuko, K., Nakata, K., Murakami, T., Nakano, R., Hara, M., Koide, Y., Suzuki, T., Ikekita, M., Morito, Y., & Fujishima, A. (2011). Development of an O₃-assisted photocatalytic water-purification unit by using a TiO₂ modified titanium mesh filter. *Catalysis Science & Technology*, 2(1), 76–78. <https://doi.org/10.1039/C1CY00315A>
- [38]. Zou, L., & Zhu, B. (2008). The synergistic effect of ozonation and photocatalysis on color removal from reused water. *Journal of Photochemistry and Photobiology A: Chemistry*, 196(1), 24–32. <https://doi.org/10.1016/J.JPHOTOCHEM.2007.11.008>
- [39]. Sun, J., Qiao, L., Sun, S., & Wang, G. (2008). Photocatalytic degradation of Orange G on nitrogen-doped TiO₂ catalysts under visible light and sunlight irradiation. *Journal of Hazardous Materials*, 155(1–2), 312–319. <https://doi.org/10.1016/J.JHAZMAT.2007.11.062>
- [40]. Sun, J., Wang, X., Sun, J., Sun, R., Sun, S., & Qiao, L. (2006). Photocatalytic degradation and kinetics of Orange G using nano-sized Sn(IV)/TiO₂/AC photocatalyst. *Journal of Molecular Catalysis A: Chemical*, 260(1–2), 241–246. <https://doi.org/10.1016/J.MOLCATA.2006.07.033>
- [41]. Chávez, A. M., Rey, A., Beltrán, F. J., & Álvarez, P. M. (2016). Solar photo-ozonation: A novel treatment method for the degradation of water pollutants. *Journal of Hazardous Materials*, 317, 36–43. <https://doi.org/10.1016/j.jhazmat.2016.05.050>
- [42]. Ranc, B., Faure, P., Croze, V., & Simonnot, M. O. (2016). Selection of oxidant doses for in situ chemical oxidation of soils contaminated by polycyclic aromatic hydrocarbons (PAHs): A review. *Journal of Hazardous Materials*, 312, 280–297. <https://doi.org/10.1016/j.jhazmat.2016.03.068>
- [43]. Bahnemann, D. (1999). Photocatalytic Detoxification of Polluted Waters. *ACS Division of Environmental Chemistry, Preprints*, 41(1), 285–351. https://doi.org/10.1007/978-3-540-69044-3_11

بهینه‌سازی فرآیند ترکیبی فتوکاتالیست - ازن برای تصفیه‌ی آب همراه

مسعود ربیعان و فرهاد قادری*

گروه مهندسی محیط زیست، دانشکده عمران، دانشگاه صنعتی نوشیروانی بابل

* نویسنده مسئول مکاتبات: F.Qaderi@nit.ac.ir

چکیده:

آب همراه یکی از پساب‌های پر خطر محیط زیست و حاوی هیدروکربن‌های چند حلقه‌ای آروماتیک است که باید به صورت مؤثر تصفیه شود. در این پژوهش یک روش نوآورانه از ترکیب فرآیند فتوکاتالیستی با استفاده از نانوذره TiO_2 ، لامپ UV و ازن ارائه شده است. پارامترهای مختلفی از جمله توان لامپ (بین ۱۰ تا ۵۰ وات)، دوز ازن (بین ۰.۱ تا ۰.۵ میلی‌گرم بر لیتر)، غلظت نانوذره (۰.۵ تا ۲.۱ گرم بر مترمربع)، درصد اتانول (۲۵ تا ۸۸ درصد)، pH (بین ۴.۵ تا ۱۰.۵)، غلظت فنانتترین (بین ۵ تا ۲۵ میلی‌گرم بر لیتر) و زمان تصفیه (۱۵ تا ۴۵ دقیقه)، برای بررسی تخریب آلاینده در آب همراه مورد بررسی قرار گرفت. در این پژوهش از روش سطح پاسخ برای مدل‌سازی و بهینه‌سازی حذف آلاینده‌ی فنانتترین استفاده شد. نتایج آزمایشگاهی منجر به ایجاد یک مدل و همچنین شرایط بهینه برای دستیابی به بیشترین راندمان حذف آلاینده‌ی فنانتترین شد. پس از پیاده‌سازی شرایط بهینه در آزمایشگاه، راندمان حذف ۹۸ درصد حاصل شد. شرایط بهینه شامل توان UV ۴۰ وات، دوز ازن ۰.۵ میلی‌گرم بر لیتر، غلظت نانوذره ۲ گرم بر مترمربع، درصد اتانول ۲۵٪، pH ۵.۲ و مدت زمان تصفیه ۴۰ دقیقه است. این رویکرد بهینه قابلیت حذف مؤثر ترکیبات چندحلقه‌ای آروماتیک را با روشی دوستدار محیط زیست، دارد.

کلمات کلیدی: فتوکاتالیست - ازن، ترکیبات چند حلقه‌ای آروماتیک، آب همراه، روش سطح پاسخ، محیط زیست پایدار.